



## ISTITUTO NAZIONALE DI RICERCA METROLOGICA Repository Istituzionale

Photonic Jets and Single-Photon Emitters

*Original*

Photonic Jets and Single-Photon Emitters / Ristori, Andrea; Felici, Marco; Pettinari, Giorgio; Pattelli, Lorenzo; Biccari, Francesco. - In: ADVANCED PHOTONICS RESEARCH. - ISSN 2699-9293. - 3:11(2022), p. 2100365. [10.1002/adpr.202100365]

*Availability:*

This version is available at: 11696/75299 since: 2023-05-12T08:53:24Z

*Publisher:*

Wiley

*Published*

DOI:10.1002/adpr.202100365

*Terms of use:*

This article is made available under terms and conditions as specified in the corresponding bibliographic description in the repository

*Publisher copyright*

(Article begins on next page)

# Photonic Jets and Single-Photon Emitters

Andrea Ristori, Marco Felici, Giorgio Pettinari, Lorenzo Pattelli, and Francesco Biccari\*

Photonic jets (PJs) obtained by illuminating a dielectric microsphere have recently shown to provide an efficient and cost-effective means of laser-writing and localizing single-photon emitters with sub-diffraction precision. The fabrication technique relies on the photoinduced formation of GaAsN quantum dots (QDs) that are self-aligned to the microsphere, which in turn enhances the collection efficiency of their emission. Similarly, the angular magnification introduced by a microsphere placed on top of two close emitters allows to detect and resolve their separation below the diffraction limit by analyzing their angular emission pattern in momentum space. Along with a brief review of the two methods, a systematic numerical study on the formation and properties of PJs to streamline the optimization of the fabrication process is presented.

## 1. Introduction

A photonic jet (PJ) consists of a highly intense electromagnetic beam with sub-wavelength lateral extent, obtained by illuminating a micrometer-sized object or microparticle with a plane or Gaussian wave. PJs have been observed with a multitude of particle shapes, including microcylinders,<sup>[1,2]</sup> microspheres,<sup>[3–5]</sup> micro-ellipsoids,<sup>[6,7]</sup> micro-cubes,<sup>[8]</sup> core-shell microspheres,<sup>[9,10]</sup> and others.<sup>[11–15]</sup> The

lateral size of a PJ can be as small as  $\lambda/3$ ,<sup>[3]</sup> and it can propagate for several wavelengths in the surrounding medium in an elongated shape with little divergence.

Since their first observation in 2004,<sup>[1]</sup> PJs have been extensively studied both from a theoretical and an experimental point of view. The use of increasingly advanced simulation techniques helped understand the dependence of the PJ's characteristics on the wavelength and polarization of the incident light,<sup>[4,16]</sup> microparticles size,<sup>[17]</sup> and their refractive index.<sup>[18]</sup> This opened the path to a better understanding of PJs and, consequently, to the possibility to engineer and exploit them in several different fields such as fluorescence spectroscopy,<sup>[19]</sup>

enhancement of Raman scattering,<sup>[20]</sup> nanoparticles sensing,<sup>[21]</sup> imaging,<sup>[22]</sup> nanolithography,<sup>[23,24]</sup> and many others.<sup>[25]</sup>

In this work, we review two applications connected to single-photon emitters and more specifically to quantum dots (QDs). The first application concerns the possibility of using PJs to laser-write GaAsN QDs,<sup>[5]</sup> while the second one relies on PJs to optically resolve the position of two emitters with sub-diffraction resolution.<sup>[26]</sup> Additionally, in this work, we perform a novel systematic study on the properties of PJs that can be obtained based on the material platform introduced in these previous works,<sup>[5,26]</sup> identifying optimal configurations for the QD fabrication process.

## 2. Fabrication of Quantum Dots

In a recent publication,<sup>[5]</sup> we introduced a laser-writing technique based on PJs as an easy and cost-effective approach to the fabrication of GaAsN QDs. We demonstrated that starting from a fully hydrogenated GaAsN:H/GaAs quantum well (QW), it is possible to locally break N–H bonds by the use of PJs, thus forming GaAsN QDs embedded in a GaAs matrix.

GaAs<sub>1-x</sub>N<sub>x</sub> is a dilute nitride semiconductor obtained by introducing a small percentage (typically less than 5%) of N in GaAs. The N presence strongly perturbs the conduction band structure, drastically reducing the bandgap.<sup>[27]</sup> The subsequent introduction of hydrogen in GaAsN, conversely, leads to the formation of stable N–H complexes, which gradually revert the effects of nitrogen, eventually restoring the bandgap, effective mass, spin properties, refractive index, lattice constant, and ordering of the N-free material.<sup>[28,29]</sup> Therefore, by controlling hydrogen diffusion within the nitride, e.g., by placing H-opaque masks on the sample,<sup>[30]</sup> it is possible to obtain small regions of low-bandgap GaAsN surrounded by high-bandgap GaAsN:H barriers, i.e., a QD. In addition, N–H bonds can be broken by illuminating hydrogenated GaAsN with a laser light of proper


A. Ristori, F. Biccari  
Department of Physics and Astronomy  
University of Florence  
Via G. Sansone 1, I-50019 Sesto Fiorentino, FI, Italy  
E-mail: francesco.biccari@unifi.it

A. Ristori, L. Pattelli, F. Biccari  
European Laboratory for Non-Linear Spectroscopy (LENS)  
University of Florence  
Via N. Carrara 1, I-50019 Sesto Fiorentino, FI, Italy

M. Felici  
Department of Physics  
Sapienza University of Rome  
Piazzale Aldo Moro 5, I-00185 Roma, Italy

G. Pettinari  
Institute for Photonics and Nanotechnologies (CNR-IFN)  
National Research Council  
Via Cineto Romano 42, I-00156 Roma, Italy

L. Pattelli  
Advanced Materials & Life Science Division  
National Institute of Metrological Research (INRiM)  
Strada delle Cacce 91, I-10135 Torino, Italy

 The ORCID identification number(s) for the author(s) of this article can be found under <https://doi.org/10.1002/adpr.202100365>.

© 2022 The Authors. Advanced Photonics Research published by Wiley-VCH GmbH. This is an open access article under the terms of the Creative Commons Attribution License, which permits use, distribution and reproduction in any medium, provided the original work is properly cited.

DOI: 10.1002/adpr.202100365

wavelength ( $500 \text{ nm} < \lambda < 800 \text{ nm}$ ).<sup>[31,32]</sup> This implies that there is another way to fabricate GaAsN QDs, i.e., by locally breaking the N–H bonds in a fully hydrogenated GaAsN:H/GaAs QW.

This approach was first tested by fabricating GaAsN QDs with the use of a scanning near-field optical microscopy (SNOM) system.<sup>[33]</sup> However, in the attempt to drastically simplify the process, we have recently managed to fabricate QDs by breaking the N–H bonds leveraging on the controlled formation of a PJ obtained illuminating SiO<sub>2</sub> microspheres deposited on top of a GaAsN:H/GaAs QW.<sup>[5]</sup> In detail, the microspheres employed had a diameter of  $(2.06 \pm 0.05) \mu\text{m}$  (the reported uncertainty is equal to one standard deviation) and they were illuminated for 1 s with a continuous wave (CW) laser at 532 nm. Control of their size was possible by tuning the laser power, as shown in **Figure 1a**. Moreover, the presence of a self-aligned microsphere right on top of the QD significantly enhances the luminescence collection efficiency of the overall system (**Figure 1b**) by a factor of  $7.3 \pm 0.7$ .<sup>[5]</sup> The resulting collection efficiency,  $\approx 14\%$ , can be compared with that reported in the literature exploiting different approaches, as summarized in **Table 1**.

The QDs fabricated with this novel technique are still characterized by a rather large homogeneous broadening of the emission ( $\approx 1 \text{ meV}$ ) and a non-perfect state purity, as seen by the fact that the background-corrected second order autocorrelation function value at zero delay is slightly less than 0.1.<sup>[5]</sup> Moreover, the observed maximum brightness, about  $7 \times 10^5 \text{ s}^{-1}$  at saturation power on the first collection lens with  $\text{NA} = 0.7$  ( $5 \times 10^6 \text{ s}^{-1}$  with the help of the microsphere), is still lower than that of other single-photon sources,<sup>[41–43]</sup> in particular, compared to the state of the art of  $1 \times 10^7 \text{ s}^{-1}$  reported, in similar condition, for InAs QDs at 4 K. Nonetheless, this technique offers also several advantages, such as: 1) working in air at room temperature, 2) drastically reducing the complexity and the costs of the fabrication process, and

**Table 1.** State-of-the-art techniques to enhance the luminescence collection of single-photon emitters (mainly QDs) with their main characteristics. Several of these approaches include a back-reflector. Also in the microsphere approach, the QW/air back interface acts as a nonoptimal back-reflector. The value of the collection efficiency is reported considering a collection optical system with a numerical aperture (NA) of 0.7. The collection efficiency of the microspheres was calculated considering that the system without the microsphere has a nominal collection efficiency of 2%.

Technique	Required spatial alignment	Required spectral matching	Collection efficiency (NA = 0.7)	Lithography required?
Microspheres (this work) <sup>[5]</sup>	Self-aligned	Broadband ( $\approx 200 \text{ nm}$ )	$\approx 14\%$	No
Fabry–Pérot microcavities <sup>[34]</sup>	Tunable	Broadband	8.6%	Yes
Photonic trumpets <sup>[35]</sup>	$\approx 20 \text{ nm}$	Broadband	95%	Yes
3D printed microlenses <sup>[36]</sup>	34 nm	Broadband	23%	Yes
Gold rings <sup>[37]</sup>	$\approx 50 \text{ nm}$	Broadband ( $\approx 70 \text{ nm}$ )	$\approx 15\%$	Yes
Photonic Crystal Cavities <sup>[38]</sup>	$< 50 \text{ nm}$	$\approx 2.5 \text{ nm}$	$\approx 44\%$	Yes
3D printed Bragg gratings <sup>[39]</sup>	50–250 nm	$\approx 70 \text{ nm}$	48%	Yes
Micropillar cavities <sup>[40]</sup>	50 nm	0.5 nm	64%	Yes

3) being reversible. Indeed, by re-hydrogenating the QW allows to “erase” the QDs thus restoring the initial conditions.

### 3. Numerical Simulations

To further optimize the fabrication process, we present the results of extensive numerical calculations studying the

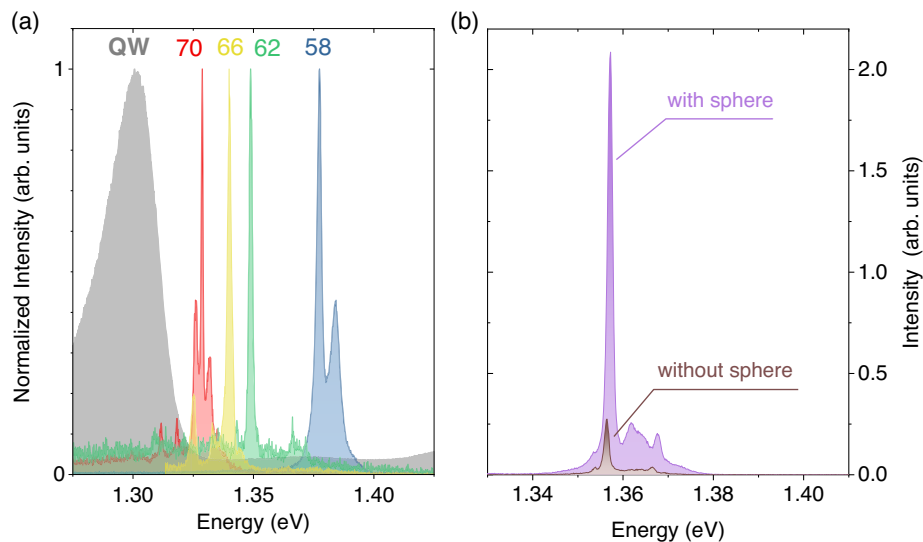


**Figure 1.** a) Photoluminescence (PL) spectra, normalized to the maximum, measured at 10 K and with a CW excitation power of 300 nW, of four different quantum dots (QDs) fabricated by photonic jet (PJ) writing in a fully hydrogenated GaAsN/GaAs quantum well (QW) at different fabrication powers, distinguished by colors. The fabrication powers, in units of mW, are provided as labels. The shaded spectrum corresponds to the PL spectrum of the GaAsN/GaAs QW before hydrogenation. b) PL spectra, measured with a CW excitation power of 500 nW, of a QD before and after removing the microsphere on top of it. The presence of the microsphere results in a approximately sevenfold enhancement of the signal (see ref. [5] for a detailed description of the enhancement estimation). Reproduced with permission.<sup>[5]</sup> Copyright 2021, Wiley-VCH.

properties of the PJs that can be formed on the selected platform. In particular, the intensities at the target depth and the full width at half maximum (FWHM) of the PJs were studied as a function of the laser wavelength and microsphere radius to identify optimal parameter combinations.

The simulations are based on a recently developed Python package named SMUTHI,<sup>[44]</sup> which combines the T-matrix method for individual particle scattering with the scattering matrix formalism for the propagation of the electromagnetic field through plane-parallel interfaces. This allows to run rigorous 3D simulations with a fraction of the memory and computational resources typically needed using common mesh-based simulation approaches. The performed simulations consist of a plane wave hitting a SiO<sub>2</sub> microsphere placed on top of a multilayer structure comprising, from bottom to top: a GaAs substrate, a 2 nm layer of Ga<sub>2</sub>O<sub>3</sub>, 1500 nm of air, another 2 nm layer of Ga<sub>2</sub>O<sub>3</sub>, a 162 nm layer of GaAs, and an additional 2 nm layer of Ga<sub>2</sub>O<sub>3</sub> (see Figure 2). The values of the refractive index of GaAs, Ga<sub>2</sub>O<sub>3</sub>, and SiO<sub>2</sub> are taken from Papatryfonos et al.,<sup>[45]</sup> Malitson,<sup>[46]</sup> and Rebien et al.,<sup>[47]</sup> respectively. This particular structure was modeled after the actual sample structure (see<sup>[5]</sup> for more details). The use of a single layer of GaAs instead of a GaAsN:H/GaAs QW is due to the fact that a fully hydrogenated GaAsN layer has the same optical properties as a GaAs layer (within 1%),<sup>[28]</sup> while the Ga<sub>2</sub>O<sub>3</sub> layers were included to account for the native GaAs oxidation process.<sup>[48]</sup> The layer structure is infinitely extended in the plane.

The parameters we are interested in are the FWHM and intensity of the PJs, which were studied as a function of the incident wavelength and the microsphere radius. In particular, we scanned wavelengths between 400 and 1550 nm in 5 nm steps and radii between 250 and 1025 nm in 25 nm steps. The results of the simulations are shown in Figure 3. The FWHM and intensity values were obtained from the electric field intensity profile

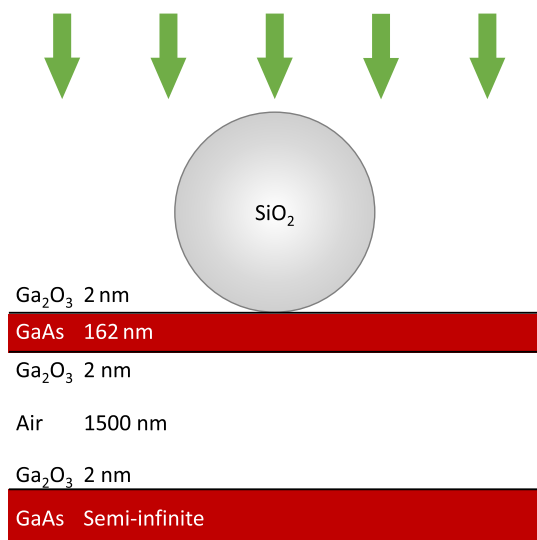


**Figure 2.** Scheme of the simulated sample, consisting of a suspended GaAs layer, an air-gap, a GaAs substrate, and a SiO<sub>2</sub> microsphere. A thin Ga<sub>2</sub>O<sub>3</sub> layer is also applied to all GaAs–air interfaces. The green arrows represent the plane wave hitting the microsphere and leading to the formation of the PJ. The drawing is not to scale.

evaluated both in the direction parallel to the polarization of the incoming plane wave and in the orthogonal one, 33 nm below the surface. This particular depth is chosen accordingly to where the GaAsN:H/GaAs QW was placed in the sample used in our previous work.<sup>[5]</sup> The results for the FWHM are shown in Figure 3a,b and are calculated with respect to the baseline intensity relative to the unperturbed plane wave illumination calculated at the same depth. In contrast, Figure 3c reports the values of the electric field intensity measured at the center of the layer, on-axis with the microsphere. The gray points in the maps represent those radius–wavelength combinations that are not associated with the formation of a PJ (i.e., the observed intensity maximum is off-axis), which would lead to the formation of the QD in a different position, or no QD formation altogether. Conversely, for all other radius–wavelength combinations, a PJ is properly formed within the GaAs layer, as we can see from Figure 3e.

In addition to that, observing the FWHM and intensity maps, the presence of an oscillating pattern immediately stands out. These oscillations can be better analyzed by plotting the quantities as a function of one of the two parameters, e.g., the wavelength, fixing the radius. As we can see from Figure 3d, these oscillations are well pronounced between 400 and 800 nm, while at longer wavelengths they are less evident. Furthermore, it is clear, e.g., looking at the dashed lines, that the oscillations of the FWHM and the intensity are exactly out of phase (maxima of the former correspond to minima of the latter, and vice versa). The origin of this behavior is likely due to the interference between the incoming wave and the ones reflected within the microsphere and by the substrate. Due to the complexity of our system, this phenomenon is not easily attributable to a single origin. However, these oscillations can be exploited when selecting the proper microsphere’s radius and laser wavelength to tune the size of laser-written QDs, taking into account the actual sample geometry, within a broad range of values. Indeed, thanks to the presence of sharp oscillations in this composite system, it is possible to strongly change the PJs behavior by slightly changing the laser wavelength, leading to an optimal control over the QDs dimension. Moreover, this effect can be combined with the control over the laser power to further increase the range of tunability. The wavelength range in which the strongest oscillations appear (400–800 nm) overlaps nicely with the operating window of commercial Ti:Sa lasers (possibly equipped with a frequency-doubling crystal, to reach the lower end of the range). Furthermore, this is the ideal wavelength range for our laser-writing applications, since the optimal wavelength for the breaking of N–H bonds in hydrogenated dilute nitrides is ≈700 nm.<sup>[32,49]</sup>

To apply the simulated results in practice, we must take into account that the microspheres are not perfectly identical; indeed, the standard deviation of their radii is about 25 nm. This inevitably leads to an uncertainty in determining the correct behavior of the oscillations, which in turn would be detrimental to the optimal control of the QDs’ size. A more detailed study of the effect of particle polydispersity is reported in the Supporting Information. To prevent this from becoming a setback for the accurate definition of the QDs’ size and emission wavelength, one should ideally determine the size of the microspheres used, e.g., with a scanning electron microscope (SEM) or an atomic

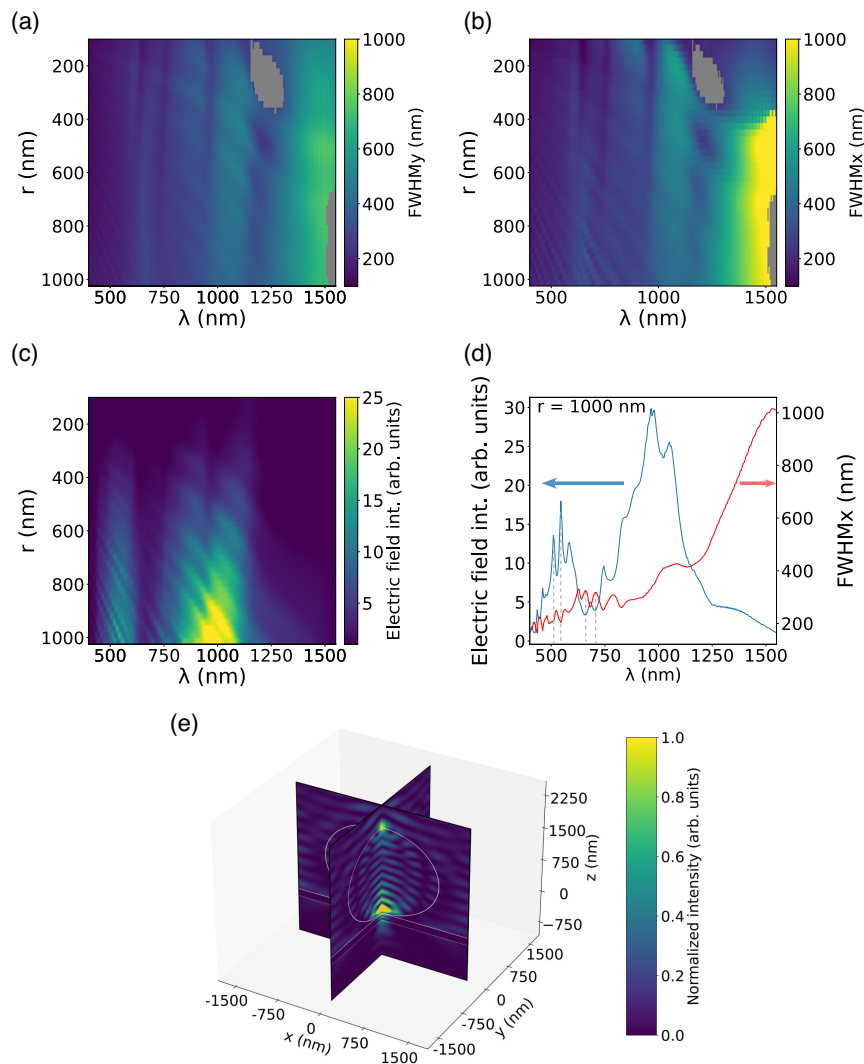


**Figure 3.** a,b) 2D maps of the FWHM of the PJ along the  $y$  and  $x$  directions, respectively, as a function of the microsphere radius and of the wavelength. The incident wave is polarized along  $y$ . c) 2D map of the electric field intensity of the PJ as a function of the microsphere radius and of the wavelength. The gray points represent those radius–wavelength combinations that are associated with an intensity minimum rather than a maximum below the microsphere. d) Plot of the FWHM (red curve) and the electric field intensity (blue curve) as a function of the wavelength for a microsphere of radius 1000 nm. The dashed lines are a guide to the eye to highlight the anti-phase behavior. e) Map of the electric field intensity in the  $xz$  and  $yz$  planes, for a microsphere of radius  $1\ \mu\text{m}$  illuminated by a plane wave with  $\lambda = 545\ \text{nm}$ . The white lines represent the contour of the microsphere and of the QW.

force microscope (AFM), thus optimizing the simulation accordingly. In this way, the identification of the laser wavelength required to obtain the desired PJs' width and intensity should be straightforward.

Regarding the ability to fabricate multiple QDs at once with a single laser pulse, we have studied the PJ properties generated by the simultaneous illumination of two adjacent microspheres (see Supporting Information). These simulations show that the properties of the two PJs are only slightly modified with respect to the single-microsphere case.

It is worth noting that, to the best of our knowledge, our systematic study of the properties of PJs as a function of particle radius and wavelength is the only one taking into account the 3D nature of the problem and the presence of a realistic

multilayer substrate. As such, we envision that these results, as well as their fast computational time, will streamline the optimization of this lithographic technique leading to a better control of QD size and positioning.

#### 4. Spatial Resolution

We now review the second application of PJs, also directly connected to single-photon emitters, which consists of the possibility to optically detect and resolve two QDs placed below a dielectric microsphere. It is well known that a PJ is formed in the shadow cone of an illuminated microsphere, and that its lateral displacement depends on the angle between the incident wave direction



and the microsphere axis defined as the normal to the substrate plane (see, e.g., Supporting Information of ref. [5]). If the two directions are parallel, the PJ will form directly on-axis with the microsphere; if there is an angle between them, the position of the PJ will be shifted accordingly. The value of the shift depends on the microsphere's properties and on the presence and characteristics of the substrate, so it must be evaluated on a case-by-case basis. However, if the wave angle is not too big, the PJ will still propagate almost parallel to the sphere axis. Interestingly, the inverse process can be used to resolve two different emitters located under the microsphere. Indeed, if we place an emitter on-axis with the microsphere, its emission will

be directed mostly vertically, while if an emitter is slightly off-axis, its emission will be beamed out of the microsphere at an angle. Therefore, by collecting the emission at different angles, we are able to resolve the presence of two or more emitters. Moreover, by analyzing the angular emission pattern, it is also possible to have an indirect measurement of the distance between them.

This idea has been tested as a part of one of our previous works<sup>[26]</sup> and the main results are shown in **Figure 4**. In detail, we measured the photoluminescence (PL) of a sample containing self-assembled GaAs QDs with SiO<sub>2</sub> microspheres on top, searching for two QDs placed below the same sphere (a detailed

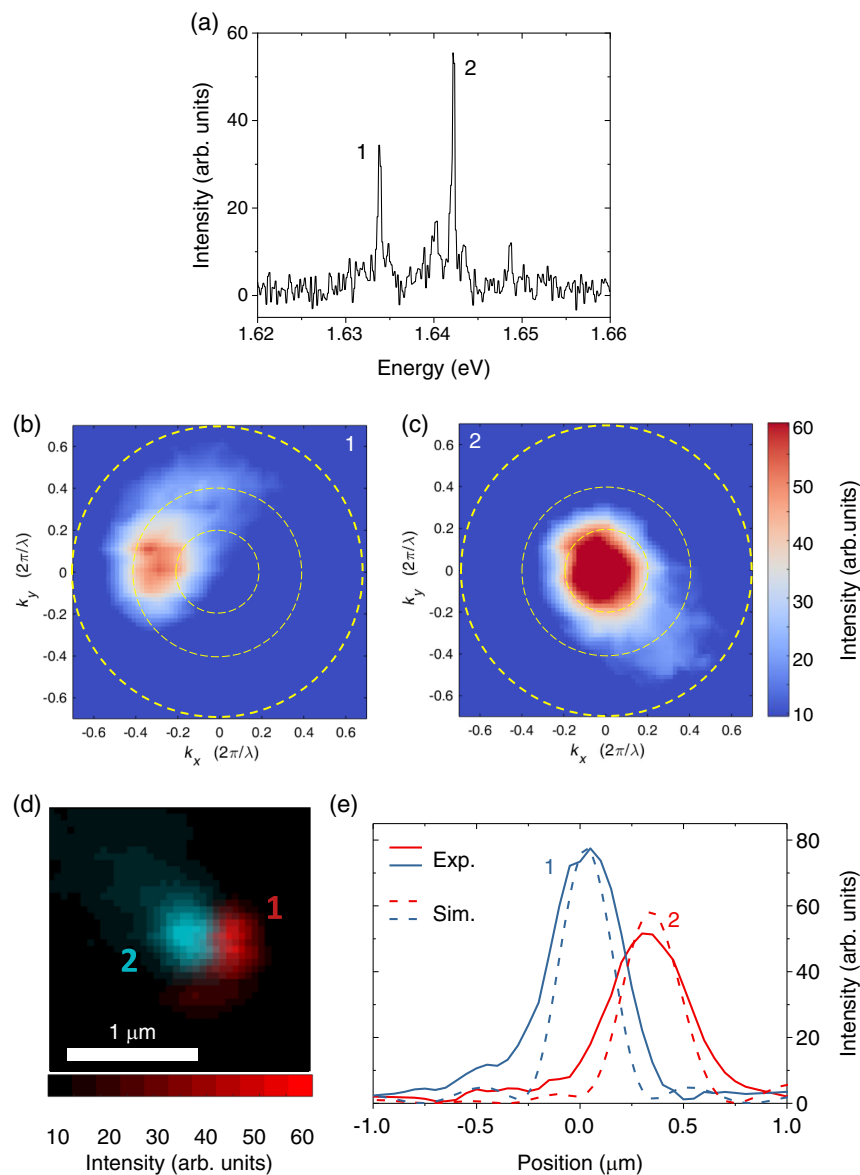


**Figure 4.** Example of use of a microsphere to distinguish the presence of two GaAs QDs underneath it. a) PL spectra of the QDs, labeled as 1 and 2. b,c)  $k$ -space maps of the PL emission of two QDs integrated over the emission energy of QD 1 and 2, respectively. The three yellow circles represent  $NA = 0.2$ ,  $NA = 0.4$ , and  $NA = 0.7$ . d) Real space map of the emission of the two QDs obtained by a transformation of the  $k$ -space maps of panels (b) and (c) (see text). e) Cuts of the map in panel (d) along the direction joining the two centers (continuous lines). The dashed lines represent the same cuts applied on the simulated spatial map. Reproduced with permission.<sup>[26]</sup> Copyright 2019, Wiley-VCH.

description of the sample is present in ref. [26]). After finding two such QDs, we measured the angular pattern of the emission of the two dots (labeled as QD1 and QD2) in  $k$ -space. Since the measurements were performed with a homemade confocal setup equipped with a  $100\times$  objective,<sup>[26]</sup> this was realized by introducing a pinhole in the collimated region of the PL signal, right after the objective. By scanning the pinhole position in the plane perpendicular to the light propagation, we could, therefore, obtain an angular (momentum  $k$ ) filter for the collected emission. A spectrum is measured for each position of the pinhole, obtaining a  $k$ -space map of the global signal. By integrating the map over the emitting energies of QD1 and QD2, we were then able to isolate the angular pattern of each dot. The results of this process are the two maps shown in Figure 4a,b. From these maps, it is clear that the signal comes from two different QDs, where QD2 is on-axis with the microsphere while QD1 is off-axis. From this measurement, it is possible to estimate the distance between the two QDs. Indeed, a transformation from the  $k$ -space to the real space can be performed using a simple geometrical model (see Supporting Information of ref. [26]), from which the following equations are obtained

$$\begin{aligned}x &= -r(k_x \tilde{\lambda})(1 - (k_x \tilde{\lambda})^2 - (k_y \tilde{\lambda})^2)^{-1/2} \\ \gamma &= -r(k_y \tilde{\lambda})(1 - (k_x \tilde{\lambda})^2 - (k_y \tilde{\lambda})^2)^{-1/2}\end{aligned}\quad (1)$$

where  $k_x$  and  $k_y$  represent the angular momentum along  $x$  and  $y$ , respectively,  $\tilde{\lambda} = \lambda/(2\pi)$  being  $\lambda$  the emission wavelength in vacuum, and  $r$  is the microsphere radius. By applying this transformation to each  $k$ -space map and then superimposing them, we obtain the real space map shown in Figure 4c, revealing an estimated inter-distance of 300 nm (see cross-cuts in Figure 4d). This result was validated numerically by performing a set of simulations for dipoles with different off-axis displacements. The best agreement between experimental and numerical profiles is again obtained for a QD in an on-axis position and one laterally displaced of 300 nm, as can be seen by the transformed  $k$ -maps cuts (dashed lines) shown in Figure 4d. This value of the resolution is perfectly consistent with theoretical evaluations available in the literature.<sup>[50]</sup> Lastly, from this result, it is possible to calculate the lower limit of the spatial resolution enhancement due to the presence of the microsphere. Indeed, considering an initial spatial resolution of about 700 nm (diffraction limit), the ability to distinguish two different QDs separated by 300 nm results in a  $2.3\times$  spatial resolution enhancement.

## 5. Conclusions

In summary, in this work, we reviewed two applications of PJs, both related to single-photon emitters, and in particular to QDs. In the first one, the PJs are exploited to directly fabricate GaAsN QDs, with the novel technique that we have previously developed.<sup>[5]</sup> A new set of simulated results was also presented to demonstrate the flexibility of PJs in the laser-writing process. In the second application, which is complementary and can be used in conjunction with the first one, we showed how PJs can be exploited to retrieve the position of one or more QDs at the same time with sub-diffraction resolution. It is worth noting that this approach can be applied also to other kinds of emitters, and not

only to QDs. These two applications illustrate the versatility of PJs, which can be used both for the fabrication of single-photon emitters and for their detection, as well as in many other areas of photonics. In conclusion, we have shown that PJs are a versatile tool for the fabrication and detection of integrated light sources; moreover, the recent availability of the SMUTHI simulation package enables an efficient streamlining of the full characterization of realistic systems, comprising both the substrate stack and the Mie resonator responsible for the formation of the PJ.

## Supporting Information

Supporting Information is available from the Wiley Online Library or from the author.

## Acknowledgements

F.B. acknowledges Fondazione Cassa di Risparmio di Firenze for funding this work within the projects SFERIQA 2020.1511, Photonic Future 2021.1508, and the PUPO project (co-funded by the University of Florence and the Italian Ministry of University and Research). L.P. acknowledges Progetto Premiale MIUR "Volume photography" and NVIDIA Corporation for the donation of a Titan X Pascal GPU. L.P. wishes to thank Amos Egel for the fruitful discussion.

## Conflict of Interest

The authors declare no conflict of interest.

## Data Availability Statement

The data that support the findings of this study are available from the corresponding author upon reasonable request.

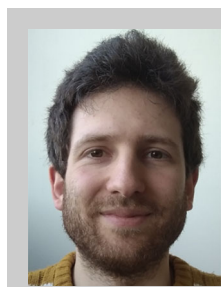
## Keywords

microspheres, photonic jets, quantum dots, single-photon emitters, T-matrix method

Received: December 8, 2021  
Revised: August 5, 2022  
Published online: August 31, 2022

- [1] Z. Chen, A. Taflove, V. Backman, *Opt. Express* **2004**, *12*, 1214.
- [2] A. V. Itagi, W. A. Challener, *J. Opt. Soc. Am. A* **2005**, *22*, 2847.
- [3] A. Heifetz, S.-C. Kong, A. V. Sahakian, A. Taflove, V. Backman, *J. Comput. Theor. Nanosci.* **2009**, *6*, 1979.
- [4] A. Mandal, V. R. Dantham, *J. Opt. Soc. Am. B* **2020**, *37*, 977.
- [5] A. Ristori, T. Hamilton, D. Toliopoulos, M. Felici, G. Pettinari, S. Sanguinetti, M. Gurioli, H. Mohseni, F. Biccari, *Adv. Quantum Technol.* **2021**, *4*, 2100045.
- [6] T. Jalali, D. Erni, *J. Mod. Opt.* **2014**, *61*, 1069.
- [7] M. Yousefi, D. Necesal, T. Scharf, M. Rossi, arXiv 2021, arXiv: arXiv:2103.17179v1, <https://doi.org/10.1364/OL.425121>.
- [8] V. Pacheco-Peña, M. Beruete, I. V. Minin, O. V. Minin, *Appl. Phys. Lett.* **2014**, *105*, 084102.
- [9] D. Grojo, N. Sandeau, L. Boarino, C. Constantinescu, N. D. Leo, M. Laus, K. Sparnacci, *Opt. Lett.* **2014**, *39*, 3989.

- [10] Y.-J. Wang, C.-A. Dai, J.-H. Li, *Polymers* **2019**, *11*, 431.
- [11] D. McCloskey, J. J. Wang, J. Donegan, *Opt. Express* **2011**, *20*, 128.
- [12] C. Zhang, J. Lin, M. Gu, *Opt. Lett.* **2021**, *46*, 3127.
- [13] Y. E. Geints, A. A. Zemlyanov, E. K. Panina, *J. Opt. Soc. Am. B* **2015**, *32*, 1570.
- [14] Z. Hengyu, C. Zaichun, C. T. Chong, H. Minghui, *Opt. Express* **2015**, *23*, 6626.
- [15] C.-B. Lin, Y.-H. Lin, W.-Y. Chen, C.-Y. Liu, *Photonics* **2021**, *8*, 334.
- [16] R. Chen, J. Lin, P. Jin, M. Cada, Y. Ma, *Opt. Commun.* **2020**, *456*, 124593.
- [17] D. Grojo, L. Boarino, N. D. Leo, R. Rocci, G. Panzarasa, P. Delaporte, M. Laus, K. Sparnacci, *Nanotechnology* **2012**, *23*, 485305.
- [18] H. Patel, P. Kushwaha, M. Swami, *Opt. Commun.* **2018**, *415*, 140.
- [19] D. Gérard, J. Wenger, A. Devilez, D. Gachet, B. Stout, N. Bonod, E. Popov, H. Rigneault, *Opt. Express* **2008**, *16*, 15297.
- [20] H. S. Patel, P. K. Kushwaha, M. K. Swami, *J. Appl. Phys.* **2018**, *123*, 023102.
- [21] X. Li, Z. Chen, A. Taflove, V. Backman, *Opt. Express* **2005**, *13*, 526.
- [22] S. Lecler, S. Perrin, A. Leong-Hoi, P. Montgomery, *Sci. Rep.* **2019**, *9*, 4725.
- [23] A. Bonakdar, M. Rezaei, R. L. Brown, V. Fathipour, E. Dexheimer, S. J. Jang, H. Mohseni, *Opt. Lett.* **2015**, *40*, 2537.
- [24] A. Jacassi, F. Tantussi, M. Dipalo, C. Biagini, N. Maccaferri, A. Bozzola, F. D. Angelis, *ACS Appl. Mater. Interfaces* **2017**, *9*, 32386.
- [25] A. Darafsheh, *J. Phys. Photonics* **2021**, *3*, 022001.
- [26] F. Biccari, T. Hamilton, A. Ristori, S. Sanguinetti, S. Bietti, M. Gurioli, H. Mohseni, *Part. Part. Syst. Character.* **2019**, *37*, 1900431.
- [27] U. Katsuhiro, S. Ikuo, H. Tatsuo, A. Tomoyuki, N. Takayoshi, *Appl. Phys. Lett.* **2000**, *76*, 1285.
- [28] *Hydrogenated Dilute Nitride Semiconductors*, (Ed: G. Ciatto), Jenny Stanford Publishing, New York **2015**, <https://doi.org/10.1201/b18296>.
- [29] R. Trotta, A. Polimeni, M. Capizzi, *Adv. Funct. Mater.* **2012**, *22*, 1782.
- [30] M. Felici, G. Pettinari, F. Biccari, A. Boschetti, S. Younis, S. Birindelli, M. Gurioli, A. Vinattieri, A. Gerardino, L. Businaro, M. Hopkinson, S. Rubini, M. Capizzi, A. Polimeni, *Phys. Rev. B* **2020**, *101*, 205403.
- [31] G. Pettinari, M. Felici, F. Biccari, M. Capizzi, A. Polimeni, *Photonics* **2018**, *5*, 10.
- [32] G. Pettinari, L. A. Labbate, M. S. Sharma, S. Rubini, A. Polimeni, M. Felici, *Nanophotonics* **2019**, *8*, 1465.
- [33] F. Biccari, A. Boschetti, G. Pettinari, F. L. China, M. Gurioli, F. Intonti, A. Vinattieri, M. Sharma, M. Capizzi, A. Gerardino, L. Businaro, M. Hopkinson, A. Polimeni, M. Felici, *Adv. Mater.* **2018**, *30*, 1705450.
- [34] D. Najer, I. Söllner, P. Sekatski, V. Dolique, M. C. Löbl, D. Riedel, R. Schott, S. Starosielec, S. R. Valentin, A. D. Wieck, N. Sangouard, A. Ludwig, R. J. Warburton, *Nature* **2019**, *575*, 622.
- [35] P. Stepanov, A. Delga, N. Gregersen, E. Peinke, M. Munsch, J. Teissier, J. Mørk, M. Richard, J. Bleuse, J.-M. Gérard, J. Claudon, *Appl. Phys. Lett.* **2015**, *107*, 141106.
- [36] M. Gschrey, A. Thoma, P. Schnauber, M. Seifried, R. Schmidt, B. Wohlfeil, L. Krüger, J. H. Schulze, T. Heindel, S. Burger, F. Schmidt, A. Strittmatter, S. Rodt, S. Reitzenstein, *Nat. Commun.* **2015**, *6*, 7662.
- [37] C. Haws, E. Perez, M. Davanco, J. D. Song, K. Srinivasan, L. Sapienza, *Appl. Phys. Lett.* **2022**, *120*, 081103.
- [38] K. H. Madsen, S. Ates, J. Liu, A. Javadi, S. M. Albrecht, I. Yeo, S. Stobbe, P. Lodahl, *Phys. Rev. B* **2014**, *90*, 155303.
- [39] L. Sapienza, M. Davanço, A. Badolato, K. Srinivasan, *Nat. Commun.* **2015**, *6*, 7833.
- [40] N. Somaschi, V. Giesz, L. D. Santis, J. C. Loredó, M. P. Almeida, G. Hornecker, S. L. Portalupi, T. Grange, C. Antón, J. Demory, C. Gómez, I. Sagnes, N. D. Lanzillotti-Kimura, A. Lematre, A. Auffeves, A. G. White, L. Lanco, P. Senellart, *Nat. Photonics* **2016**, *10*, 340.
- [41] I. Aharonovich, D. Englund, M. Toth, *Nat. Photonics* **2016**, *10*, 631.
- [42] S. Tamariz, G. Callsen, J. Stachurski, K. Shojiki, R. Butté, N. Grandjean, *ACS Photonics* **2020**, *7*, 1515.
- [43] X. He, N. F. Hartmann, X. Ma, Y. Kim, R. Ihly, J. L. Blackburn, W. Gao, J. Kono, Y. Yomogida, A. Hirano, T. Tanaka, H. Kataura, H. Htoon, S. K. Doorn, *Nat. Photonics* **2017**, *11*, 577.
- [44] A. Egel, K. M. Czajkowski, D. Theobald, K. Ladutenko, A. S. Kuznetsov, L. Pattelli, *J. Quant. Spectrosc. Radiat. Transfer* **2021**, *273*, 107846.
- [45] K. Papatryfonos, T. Angelova, A. Brimont, B. Reid, S. Guldin, P. R. Smith, M. Tang, K. Li, A. J. Seeds, H. Liu, D. R. Selviah, *AIP Adv.* **2021**, *11*, 025327.
- [46] I. H. Malitson, *J. Opt. Soc. Am.* **1965**, *55*, 1205.
- [47] M. Rebien, W. Henrion, M. Hong, J. P. Mannaerts, M. Fleischer, *Appl. Phys. Lett.* **2002**, *81*, 250.
- [48] B. Schwartz, *CRC Crit. Rev. Solid State Sci.* **1975**, *5*, 609.
- [49] N. Balakrishnan, G. Pettinari, O. Makarovskiy, L. Turyanska, M. W. Fay, M. D. Luca, A. Polimeni, M. Capizzi, F. Martelli, S. Rubini, A. Patané, *Phys. Rev. B* **2012**, *86*, 155307.
- [50] A. Darafsheh, *J. Appl. Phys.* **2022**, *131*, 031102.



**Andrea Ristori** is a Ph.D. student at the European Laboratory for Non-Linear Spectroscopy (LENS) of the University of Florence. His main research activity focuses on single-photon emitters, such as quantum dots and point defects in crystals, from their fabrication to their optical characterization.





**Marco Felici** is an associate professor at the Physics Department of Sapienza University of Rome (Italy). He received his Ph.D. in materials science in 2007, and he worked for 4 years (2007–2011) as a postdoctoral researcher in the Laboratory of Physics of Nanostructures at the Ecole Polytechnique Fédérale de Lausanne (EPFL, Switzerland). His research focuses on the investigation of the optical properties of low-dimensional systems, on their integration with photonic structures, and on the study of the effects of hydrogen irradiation on the properties of semiconductors.



**Giorgio Pettinari** is a staff researcher at the Institute for Photonics and Nanotechnologies of the National Research Council of Italy. He received his Ph.D. in materials science from Sapienza University of Rome (Italy, 2008), and was an assistant researcher at the High Field Magnet Laboratory of the Radboud University of Nijmegen (The Netherlands, 2009–2011) and a Marie Curie research fellow at the University of Nottingham (UK, 2011–2013). His research interests range from the experimental investigation (optics, transport, surface probe microscopies) to the micro- and nanofabrication of low-dimensional systems, photonic and plasmonic devices, as well as of detector arrays for astrophysical applications.



**Lorenzo Pattelli** is a researcher at the Istituto Nazionale di Ricerca Metrologica (INRiM) in Turin, Italy. He received his Ph.D. in atomic and molecular spectroscopy from the European Laboratory for Non-Linear Spectroscopy (LENS) of the University of Florence. His main research interests include disordered photonics, radiative transport, bioinspired materials, and scattering media. He contributed to the development of open-source software tools for optical simulations.



**Francesco Biccari** is an associate professor at the Physics and Astronomy Department of the University of Florence (Italy). He received his Ph.D. in physics in 2010 from Sapienza University of Rome (Italy). His research activity is mainly focused on the optical characterization of semiconductor nanostructures and semiconductor defects for applications in quantum information technologies and photovoltaics.